Electronic Supplementary Information for

Controllable Synthesis of Hierarchical Nickel Hydroxide Nanotubes for High Performance Supercapacitors

Yanbing Wang [a], Bin Shang [a], Feng Lin[a], Yu Chen [a], Ruguang Ma[b*],Bo Peng,[c] and Ziwei Deng [a*]

a Key Laboratory of Applied Surface and Colloid Chemistry, Ministry of Education, Shaanxi Key Laboratory for Advanced Energy Devices, Shaanxi Engineering Lab for Advanced Energy Technology, School of Materials Science and Engineering, Shaanxi Normal University, Xi'an, 710119, China.

b State Key Laboratory of High Performance Ceramics and Superfine Microstructure, Shanghai Institute of Ceramics, Chinese Academy of Sciences, 1295 Dingxi Road, Shanghai 200050, China.

c Department of Chemistry, Physical and Theoretical Chemistry Laboratory, University of Oxford, South Parks Road, Oxford OX1 3QZ, United Kingdom.

Corresponding authors:

* Dr. Ziwei Deng, E-mail: zwdeng@snnu.edu.cn

* Dr. Ruguang Ma, E-mail: maruguang@mail.sic.ac.cn

S1. Experimental Section

Materials

All chemicals were of analytic grade mentioned otherwise. Triblock copolymer Pluronic F-127 ($EO_{100}PO_{70}EO_{100}$, EO=ethylene oxide, PO=propylene oxide) were purchased from Sigma-Aldrich without further purification. Nickel nitrate hexahydrate ($Ni(NO_3)_2 \cdot 6H_2O$, ≥99.8%) tetraethyl orthosilicate (TEOS, ≥99.8%), hexadecyltrimethyl-ammonium bromide(CTAB, ≥99.8%), hydrochloric acid (HCl, 36.0–38.0%), aqueous ammonia (28 wt% aqueous solution), absolute ethanol were purchased from Sinopharm Chemical Reagent Co., Ltd (China). Ultrapure water (>17 $M\Omega cm^{-1}$) obtained from a GZY-P10 water system was used throughout experiments.

Synthesis of mesoporous SiO_2 nanorods

Mesoporous silica nanorods were synthesized by using CTAB and F-127 as the binary templates in a basic aqueous solution according to the reported procedures. In detail, all of F127(1.26g), CTAB(100mL aqueous solution, 0.04 M) and aqueous ammonia solution (120mL, 2.5wt%) were first mixed together to form a clear mixture at room temperature. TEOS (4.8 mL) was then added into the above mixture under a stir. After 10 min of stirring, the mixture was allowed to stay standing at room temperature for 6 h. The mixture gradually turned to become cloudy. The SiO_2 nanorods were collected by centrifugation and washed with ethanol and deionized water for three times. And the mesoporous channels filled with the surfactant molecules were removed by heating the SiO_2 nanorods in an ethanol/hydrochloric acidic solution at 90 ^oC for 24h. Finally, the mesoporous SiO_2 nanorods were washed with ethanol and dried in a vacuum oven for 24h.

Synthesis of nickel hydroxide nanotubes

The typical strategy used for the fabrication of nickel hydroxide nanotubes is illustrated in Scheme 1. Typically, the stock dispersion was first prepared by dispersing the mesoporous silica nanorods powder (0.1 g) into 30mL of H_2O/ethanol mixture (1:2, v/v). Subsequently, $Ni(NO_3)_2 \cdot 6H_2O$ (0.8g) was added into the above dispersion with ultrasound sonication. After that, the above dispersion was translated into a Teflon-lined stainless steel autoclave and heated at 200 ^oC in an oven for different reaction times (6h, 12h, 18h, and 24h,) respectively. After cooling down to room temperature, the nickel hydroxide nanotubes were collected by centrifugation and washed with ethanol and deionized water for several times before drying in a vacuum oven for 24h.

Characterization

The morphologies of SiO_2 nanorods and $Ni(OH)_2$ nanotubes were examined with a transmission electron microscope (TEM, JEOL JEM-2100, Japan). All samples were diluted with ethanol, ultrasonicated at 25 ^oC for 10 min, and dried onto the carbon-coated copper grids before examination. Scanning electron microscopy (SEM, Hitachi S-4800, Hitachi, Ltd. Japan) was also used to characterize the surface morphologies of the $Ni(OH)_2$ nanotubes. All dispersions were diluted with ethanol and dried on the silica wafers at room temperature before observation. Nitrogen adsorption/desorption isotherms of mesoporous SiO_2 nanorods and $Ni(OH)_2$ nanotubes were obtained from a QUADRASORB SI-4 Analyzer (Quantachrome Instruments, USA) at 77K. All the samples were degassed for 12 hours prior to the BET measurement. The specific surface area was determined with a multipoint BET method, and the pore size distribution was calculated from desorption isotherms by using the Barrett-Joyner-Halenda method. Powder X-ray

diffraction of $Ni(OH)_2$ nanotubes was performed on a DX-2700 X-ray diffractometer equipped with a Cu tube and a diffracted beam curved graphite monochromator operated at 40 kV and 30 mA. The XRD patterns were recorded by scanning the $Ni(OH)_2$ nanotubes deposited on a glass substrate with a scanning rate of 0.02 degrees (2θ) per second in the range of 10°and 80°(2θ).

Electrochemical tests

The working electrodes were prepared via mixing the electroactive materials (80 wt %), carbon black (15 wt %) and polymer binder (polyvinylidene fluoride; PVDF, 5 wt %). Then the slurry was spread on a piece of nickel foam at 10MPa as current collector and was dried at 120 °C for 12 h in vacuum. Tens of cyclic voltammetry cycles are necessary to activate the electrode materials in electrolyte before testing. For the three-electrode measurement, Pt foil was used as counter electrode and a standard calomel electrode (SCE) as the reference electrode. Cyclic voltammetry (CV) was used at different sweep rates to determine the electrochemical properties of the fabricated $Ni(OH)_2$ electrode in 6 M KOH and to quantify its specific capacitance. CV and galvanostatic charge-discharge tests were carried out on CHI 660C electrochemical analyzer (CH Instruments, Shanghai, Chenghua Co.) at room temperature. The cyclic voltammograms (CVs) were recorded in the potential range between -0.15 and 0.45 V vs. SCE at the various scan rates of 5, 10, 20 and 50 mV/s and the current responses were measured. The specific capacitances based on CV curves were calculated according to the following equation[S1]:

$$C = \frac{1}{2} \cdot \frac{\int i \cdot dV}{v \cdot m \cdot \Delta V}$$

where $\int i \cdot dV$ is the area of the CV curves within the assigned potential range, i is the response current (A), V is the potential (V), υ is the scan rate (mV/s), and m is the mass of active

materials in the electrodes (g). Galvanostatic charge/discharge tests were performed in the potential range between -0.15 V and 0.45 V vs. SCE at a current density of 1, 3, 6, 12, 20 A/g respectively. These curves were also employed to the specific capacitances according to the following equation[S2]:

$$C = \frac{I \cdot \Delta t}{m \cdot \Delta V}$$

where I (A) is the charge or discharge current, Δt (s) is the discharge time, m (g) is the mass of electroactive materials in the electrodes, and ΔV (V) is the potential window.

S2. Supporting Figures

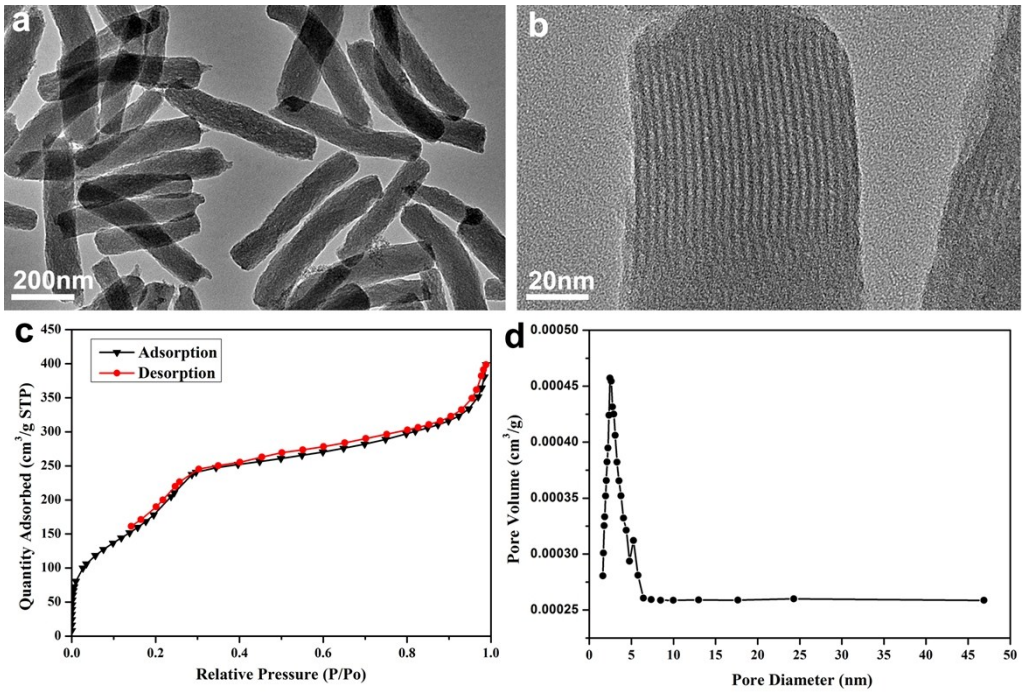

Fig.S1 Transmission electron microscopy (TEM) images of (a) mesoporous SiO_2 nanorods and (b) samples in (a) at a high magnification; (c) nitrogen-adsorption-desorption isotherms and (d) Barrett-Joyner-Halenda (BJH) pore-size-distribution of mesoporous SiO_2 nanorods.

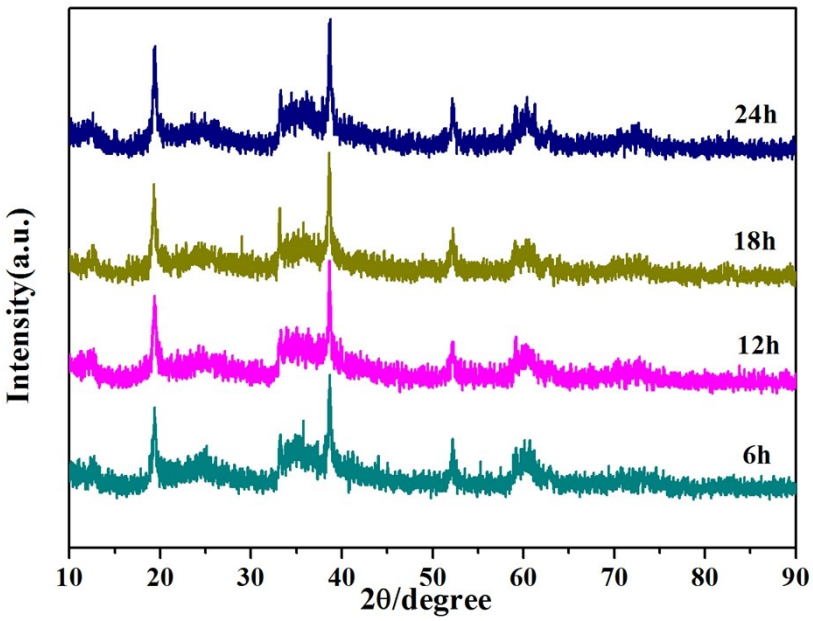

Fig.S2 X-ray diffraction (XRD) patterns of the as-produced $Ni(OH)_2$ nanotubes obtained at different reaction times: (a) 6h, (b) 12h, (c) 18h, (d) 24h.

.

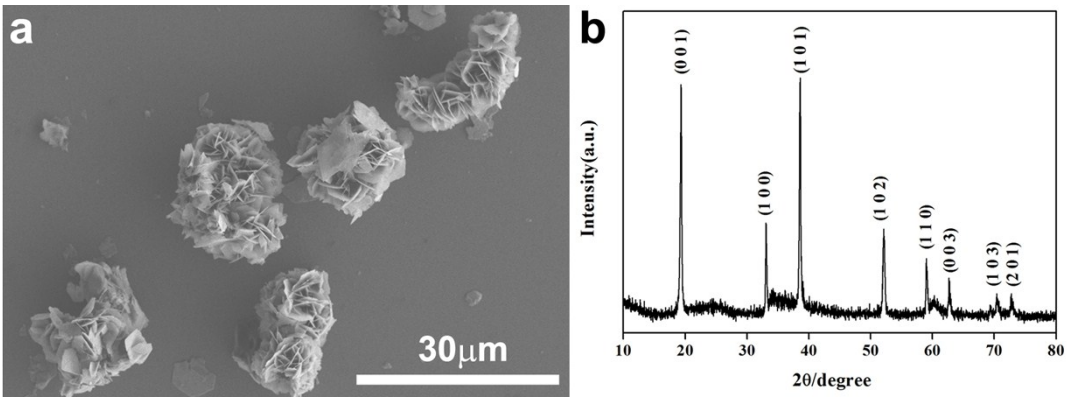

Fig.S3 (a) SEM image and (b) XRD pattern of the $Ni(OH)_2$ aggregations prepared in H_2O/ethanol mixture (1:2, v/v) after solvothermal treatment at 180 ^oC for 24h.

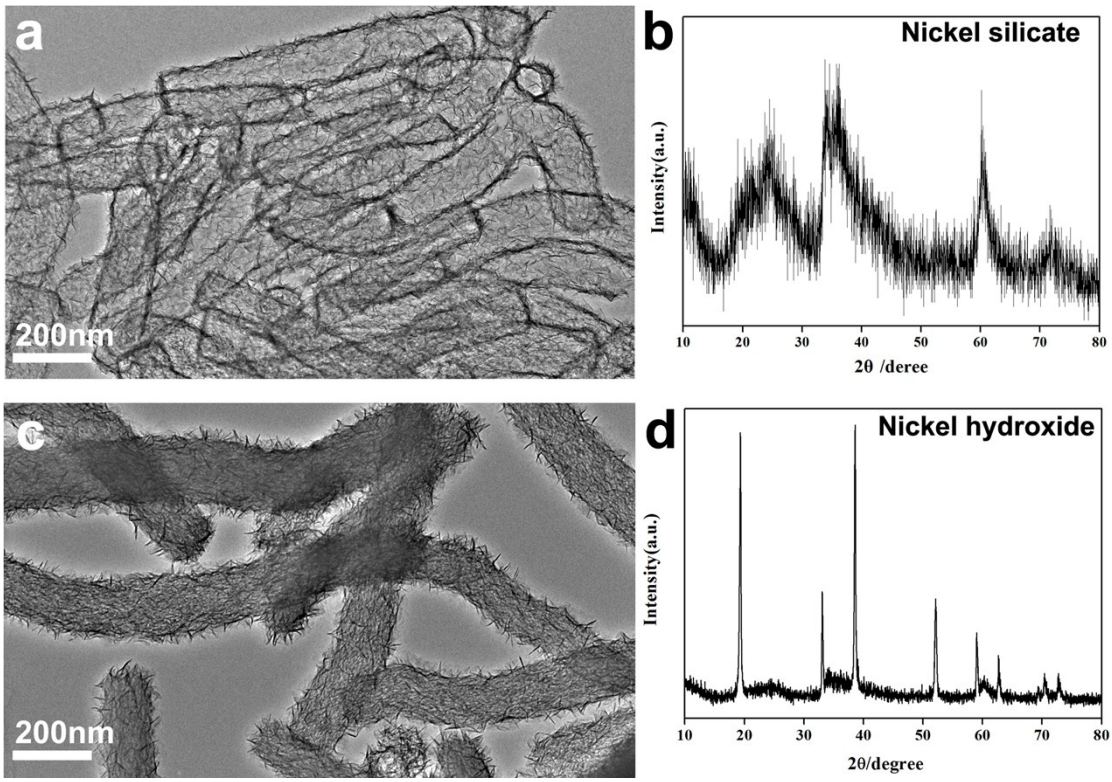

Fig.S4 TEM images and XRD patterns of (a,b) hollow nickel silicate nanotubes produced in the water media and (c,d) core-shell SiO_2@$Ni(OH)_2$ nanorods produced in ethanol media after thermal treatment at 180 ^oC for 24h.

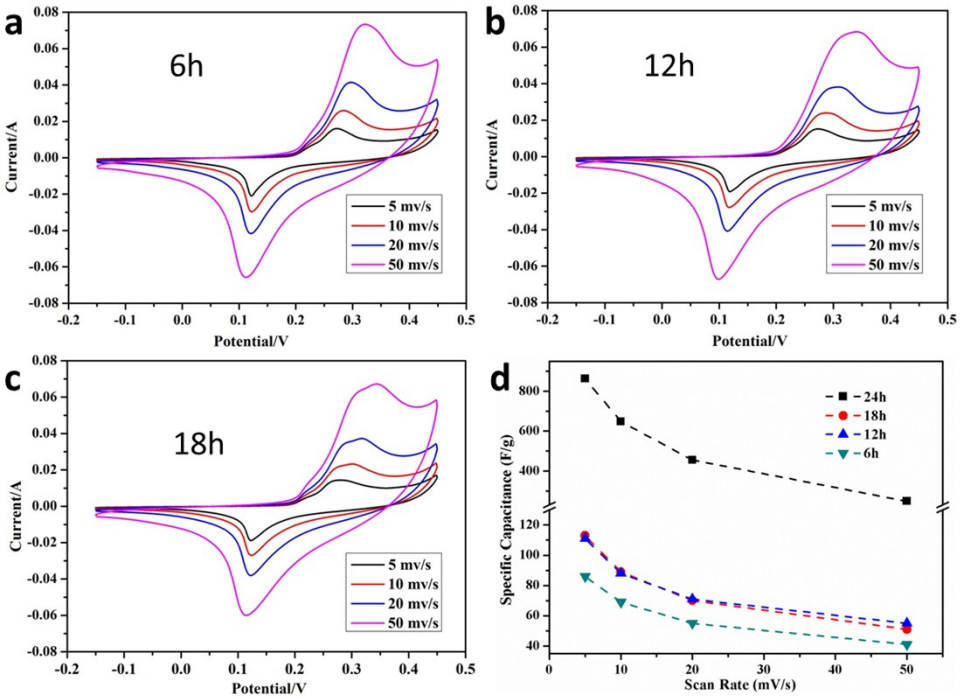

Fig.S5 (a) Cyclic voltammogram of the products obtained by the reactions after (a) 6h, (b) 12h, and (c) 18h, respectively, at various scan rates; (d) Comparison of the specific capacitance of the products obtained after different reaction time intervals.

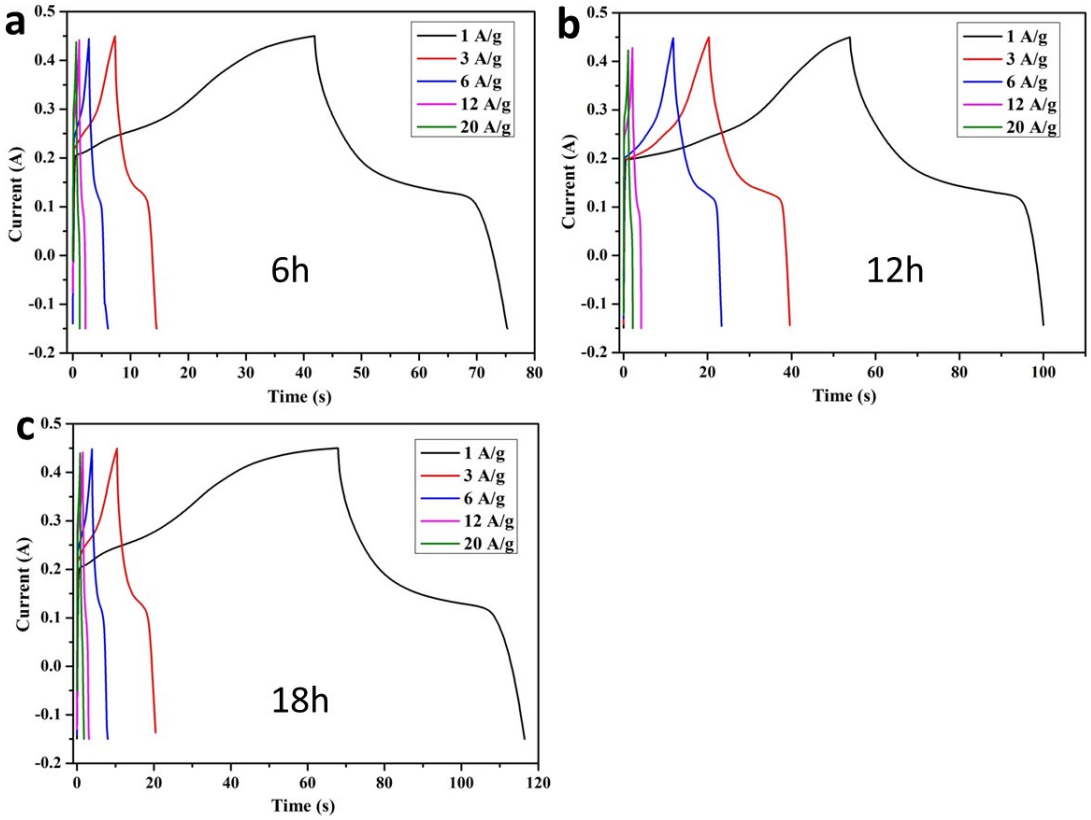

Fig.S6 Galvanostatic charge/discharge curves at different current densities of $Ni(OH)_2$ produced through the reactions of 6h, 12h, and 18h, respectively.

Table S1. Capacitance and retention of previously reported $Ni(OH)_2$-based electrodes for supercapacitors.

Electrode	Specific Capacitance	Retention	Reference
$Ni(OH)_2$ nanotubes	1319 F/g at 3 A/g 575.3 F/g at 20 A/g	79.3% after 7000 cycles at 5 A/g	This work
$Ni(OH)_2$ nanowire-MnO_2 nanoflakes @Core-shell nanostructures	487.4 F/g at 1 A/g	97.1 % after 3,000 cycles	S3
$Ni(OH)_2$ sheet on Ni foam	2384 F/g at 1 A/g	75 % after 3,000 cycles	S4
3D $Ni(OH)_2/MnO_2$/CNT on Ni foam	2,648 F/g at 1 A/g	78.2 % after 3,000 cycles	S5
$Ni(OH)_2$ on flexible 3D-Ni	3498 F/g at 10 A/g	74 % after 1,000 cycles	S6
3D Ultrathin $Ni(OH)_2$ on Graphite foam	1560 F/g at 0.5 A/g	63.2 % after 10,000 cycles	S7
$Ni(OH)_2$-CFG	167 F/g at 3 A/g	100% after 1000 cycles, at 5 A/g	S8
Nano-$Ni(OH)_2$/C	350.3 F/g at 10 A/g 349.5 F/g at 20 A/g	97% after 20000 cycles at 30 A/g	S9
Amorphous $Ni(OH)_2$	259 F/g at 20 A/g	76%, after 10000 cycles, 100 mV/s	S10
$Ni(OH)_2$/f-XC-72	1596 F/g at 1 A/g	91.3% after 1000 cycles at 10 A/g	S11
Flower-like $Ni(OH)_2$	2225.1 F/g at 0.5 A/g	111.4% after 10,000 cycles at 5 A/g	S12
Porous $Ni(OH)_2$ Nanocubes	1842 F/g at 1 A/g	80.6% after 1000 cycles at 8 A/g.	S13
$Ni(OH)_2$/CNT/rGO	633 F/g at 1 A/g	80% after 3000 cycles at 2 A/g	S14

References

S1. Y. Liu, Z. J. Shi, Y. F. Gao, W. D. An, Z. Z. Cao and J. R. Liu, *ACS Appl. Mater. Interfaces*, 2016, **8**, 28283-28290.

S2. R. Ma, Y. Zhou, L. Yao, G. Liu, Z. Zhou, J. M. Lee, J. Wang, Q. Liu, *J. Power Sources*, 2016, **303**, 49-56.

S3. H. Jiang, C. Li, T. Sun, J. Ma, *Chem. Commun.*, 2012, **48**, 2606-2608.

S4. X. Xiong, D. Ding, D. Chen, G. Waller, Y. Bu, Z. Wang, M. Liu, *Nano Energy*, 2015, **11**, 154-161.

S5. J. Shen, X. Li, L. Wan, K. Liang, B.K. Tay, L.B. Kong, X. Yan, *ACS Appl. Mater. Interfaces*, 2017, **9**, 668-676.

S6. S.I. Kim, J.H. Kang, S.W. Kim, J.H. Jang, *Nano Energy*, 2017, **39**, 639-646.

S7. J. Ji, L.L. Zhang, H. Ji, Y. Li, X. Zhao, X. Bai, X. Fan, F. Zhang, R.S. Ruoff, *ACS nano*, 2013, **7**, 6237-6243.

S8. L.L. Zhang, H.H. Li, C.Y. Fan, K. Wang, X.L. Wu, H.Z. Sun, J.P. Zhang, *J. Mater. Chem. A*, 2015, **3** 19077-19084.

S9. Y. Nie, H. Yang, J. Pana, W. Li, Y. Sun, H. Niu, *Electrochim. Acta*, 2017, **252**, 558-567.

S10. H.B. Li, M.H. Yu, F.X. Wang, P. Liu, Y. Liang, J. Xiao, C.X. Wang, Y.X. Tong, G.W.Yang, *Nat. Commun.,* 2013, **4**, 54-56.

S11. X. Qin, S. Tang, J. Yuan, Y. Deng, R. Qu, L. Wu and J. Li, *New J. Chem.*, 2017, **41**, 11372-11382.

S12. W. Wei, W. Chen, L. Ding, S. Cui, and L. Mi, *Nano Res.*, 2017, **10**, 3726-3742.

S13. L. Li, L. Tan, G. Li, Y. Zhang, and L. Liu, *Langmuir*, 2017, **33**, 12087-12094.

S14. Y. Zhang, L. Sun, K. Lv, Y. Zhang, *Mater. Lett.*, 2018, **213**, 131-134.